# Three-dimensional polarimetric integral imaging under low illumination conditions

**XIN SHEN[1], ARTUR CARNICER[2] AND BAHRAM JAVIDI[1,*]**

[1]*Electrical and Computer Engineering Department, University of Connecticut, Connecticut 06269-4157, USA*
[2]*Universitat de Barcelona (UB), Facultat de Física, Department de Física Aplicada, Martí i Franquès 1, 08028 Barcelona, Catalunya, Spain*
**Corresponding author: Bahram.Javidi@uconn.edu*

Received XX Month XXXX; revised XX Month, XXXX; accepted XX Month XXXX; posted XX Month XXXX (Doc. ID XXXXX); published XX Month XXXX

**Conventional polarimetric imaging may perform poorly in photon-starved environments. In this letter, we demonstrate the potential of integral imaging and dedicated algorithms for extracting three-dimensional (3D) polarimetric information in low light, and reducing the effects of measurement uncertainty. In our approach, the Stokes polarization parameters are measured and statistically analyzed in low illumination conditions through 3D reconstructed polarimetric images with dedicated algorithms to improve Signal-to-Noise Ratio (SNR). 3D volumetric Degree of Polarization (*DoP*) of the scene are calculated by statistical algorithms. We show that the 3D polarimetric information of the object can be statistically extracted from the Stokes parameters and 3D *DoP* images. Experimental results along with novel statistical analysis verify the feasibility of the proposed approach for polarimetric 3D imaging in photon-starved environments, and show that it outperforms its 2D counterpart in terms of SNR. To the best of our knowledge, this is the first report of novel optical experiments along with novel statistical analysis, and dedicated algorithms to recover 3D polarimetric imaging signatures in low light.**


http://dx.doi.org/10.1364/OL.99.099999

Polarization state of light contains optical and physical properties of specific materials [1]. Compared with conventional imaging, polarimetric imaging can reveal additional information of the scene and it has the potential for material inspection and classification in various applications. Three-dimensional (3D) integral imaging (InIm) [2-4] is a promising approach for 3D applications. A conventional InIm system utilizes a two-dimensional (2D) camera with a lenslet array to obtain intensity and directional information of a scene (elemental images) from multiple perspectives. The 3D reconstruction can be performed optically or computationally [1-3]. InIm has been applied for 3D displays, object recognition, augmented reality, and imaging under degraded conditions [1-3].

We investigate a 3D polarimetric InIm approach for extracting polarimetric information in low illumination conditions, and show that it outperforms its 2D counterpart. A series of 2D polarimetric intensity elemental images are first obtained by a moving polarimetric image sensor. In photon-starved environments, the 2D images and polarimetric parameters may be dominated by camera noise and are randomized. To recover the polarimetric information, the camera offset is first removed from the perspective 2D images, and then 3D images are reconstructed by dedicated statistical algorithms. In the 3D reconstruction process, the effect of camera read noise is reduced because InIm reconstruction is optimum in maximum likelihood sense [4]. The 3D polarimetric images with reduced camera offset and read noise is used to measure the Stokes polarization parameters and calculate 3D Degree of Polarization (*DoP*) of the scene. The statistical distribution of the *DoP* in low light is derived and analyzed, and total variation denoising algorithm is further applied to the *DoP* images to enhance SNR and visualization. Experimental results in low illumination and statistical analysis show that the 3D *DoP* image can be recovered with improved SNR, and 3D polarimetric information can be statistically extracted from the Stokes parameters as verified by the Kullback-Leibler Divergence [5] and Entropy metrics computation and analysis.

To perform polarimetric imaging, the Stokes polarization parameters [$S_i$, $i$=(0, 1, 2, 3)] are measured by placing a linear polarizer and quarter waveplate in front of an image sensor [Fig. 1(c)] for capturing polarimetric intensity images:

$$\begin{cases} S_0 = E_{0x}^2 + E_{0y}^2 = I^{0^\circ} + I^{90^\circ} \\ S_1 = E_{0x}^2 - E_{0y}^2 = I^{0^\circ} - I^{90^\circ} \\ S_2 = 2E_{0x}E_{0y}cos\delta = I^{45^\circ} - I^{135^\circ} \\ S_3 = 2E_{0x}E_{0y}sin\delta = I^{45^\circ,\pi/2} - I^{135^\circ,\pi/2} \end{cases}, \quad (1)$$

where $E_{0x}$ and $E_{0y}$ are the time averaged amplitudes of the $x$ and $y$ components of the electric field, and $\delta$ is the phase factor of plane wave. $I^{\alpha^\circ}$ denotes the polarimetric image when a linear polarizer with a reference angle $\alpha^\circ$ is attached to the sensor. $I^{\alpha^\circ,\pi/2}$ indicates an additional quarter waveplate is used for measuring the circular polarimetric component $S_3$. Note that $I$ represents ideal polarimetric image without the effect of camera noise. The Degree of Polarization is defined as $DoP = \left(\sqrt{S_1^2 + S_2^2 + S_3^2}\right)/S_0$, where *DoP* is between

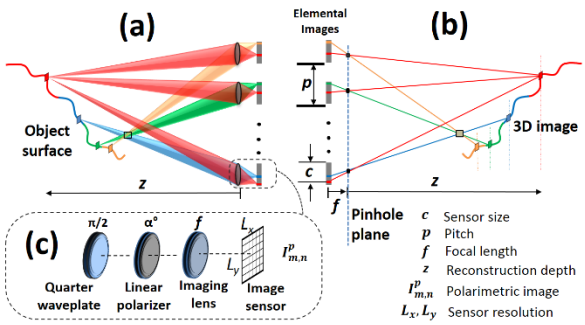


Fig. 1. SAII based 3D polarimetric imaging. (a) 3D sensing, (b) computational reconstruction, and (c) polarimetric imaging.

[0, 1] without noise. The *DoP* can be decomposed into the Degree of Linear Polarization (*DoLP*): $DoLP = \sqrt{S_1^2 + S_2^2}/S_0$, and the Degree of Circular Polarization (*DoCP*): $DoCP = |S_3|/S_0$. 3D polarimetric InIm has been shown in [6], and a numerical simulation approach for obtaining 3D polarimetric InIm with photon counting model for low light condition is presented in [7] without optical experiments and without consideration of measurement uncertainty due to camera noise. Our proposed approach substantially reduces the measurement uncertainty of polarimetric information in low light.

Synthetic Aperture Integral Imaging (SAII) [8], that is a moving camera equipped with optical polarimetric components [Fig. 1(c)] is used to experimentally investigate low light 3D polarimetric InIm. In photon-starved environments, due to the low number of photons, the captured images are dominated by camera noise, $I' = I + n$, where $I$ is the ideal 2D image generated by the photons in the scene, and $n$ is camera noise, which includes camera offset ($N_{offset}$), read noise, and dark noise etc. For low light polarimetric imaging, $N_{offset}$ to be carefully considered. The camera offset corresponds to the sensor electrons, and it is useful to prevent the clipping of small signals into a zero / negative digitized intensity, due to noise. However, in photon-starved environments the electron counts due to object are much lower than $N_{offset}$ resulting in noisy images which degrade the accuracy of *DoP* calculation.

To overcome this limitation, we first subtract the camera offset from the captured images. $N_{offset}$ is calculated by averaging a large number of single camera bias reference frames: $N_{offset} = \frac{1}{K}\sum_{k=1}^{K} bias_k$. The bias reference frames ($bias_k$, $k$=1, 2, ..., $K$) are obtained by setting the image sensor with a minimum exposure time and with a maximum f-stop (entrance pupil = 0) to avoid photons from the scene arriving at the sensor. The 2D elemental images without camera offset are:

$$\xi_{m,n}^{p} = I_{m,n}^{p} + \varepsilon, \qquad \textbf{(2)}$$

where $I_{m,n}^{p}$ is the ($m$, $n$)-th ideal polarimetric 2D image due to the photons from the scene, $p$ represents the polarimetric components [$\alpha°$ or ($\alpha°$, $\pi/2$)], and $\varepsilon$ is additive camera noise. The electronic components in the camera introduce uncertainty in the measured signal referred to as read noise, which will be the dominant noise in low light images. Also, the image may contain dark current noise because the exposure time is not zero. Dark noise is much smaller than read noise in low light levels. To further reduce the read noise, the 2D perspective images ($\xi_{m,n}^{p}$) without camera offset are used for 3D reconstruction [Fig. 1(b)] based on the SAII algorithm [8]:

$$R_z^p(x,y) = \frac{1}{O(x,y)}\sum_{m=0}^{M-1}\sum_{n=0}^{N-1}\left[I_{m,n}^{p}\left(x - \frac{m\times L_x\times p_x}{c_x\times z/f}, y - \frac{n\times L_y\times p_y}{c_y\times z/f}\right) + \varepsilon\right], \textbf{(3)}$$

where $(x, y)$ is the image pixel index, $z$ is the reconstructed depth, and $f$ is the lens focal length. $O(x,y)$ is the overlapping pixel number on $(x, y)$, and $M$ and $N$ are the total number of perspectives in the horizontal and vertical directions, respectively. $L_x$ and $L_y$ are the resolution of camera sensor. ($c_x$, $c_y$) and ($p_x$, $p_y$) are the sensor size and pitch between adjacent sensors, respectively. The pixel intensity in a 3D image ($R_z^p$) reconstructed at depth $z$ can be determined based on the maximum likelihood estimation by taking the derivative of log likelihood of the probability density function. Under low illumination conditions, the 2D image is read noise dominated with a Gaussian distribution. The corresponding probability density function is $R \sim N(\mu, \sigma^2)$. The mean value $\hat{\mu}_z^p(x,y)$ of the 3D polarimetric image can be estimated by maximizing the log likelihood estimation [4]:

$$\hat{\mu}_z^p(x,y) = \frac{1}{M\times N}\sum_{m=0}^{M-1}\sum_{n=0}^{N-1}\xi_{m,n}^{p}(x',y'), \qquad \textbf{(4)}$$

where $x' = x - \frac{m\times L_x\times p_x}{c_x\times z/f}, y' = y - \frac{m\times L_y\times p_y}{c_y\times z/f}$. The 3D reconstruction is optimum in the maximum likelihood sense given the presence of camera noise due to low light conditions. The intensity value $\hat{\mu}_z^p(x,y)$ at pixel $(x, y)$ is averaged from the 2D perspective images, which takes the same form as the SAII reconstructed image $R_z^p$. We apply SAII for the optimized 3D polarimetric image ($R_z^p$) to further reduce read noise. The 3D Stokes parameters and 3D *DoP* image of the scene can be calculated to extract the polarimetric and depth information of the scene.

We propose a statistical approach to extract 3D polarimetric information from *DoP* in low illumination. The 3D image ($R_z^p$) intensities in non-polarimetric areas and out-of-focus areas are not sensitive to the polarizer. The derived 3D Stokes parameters ($S_i^z$, $i$=[1, 2, 3]) [Eq. 1], are read noise dominated with a zero mean Gaussian [$N(0, \sigma^2)$]. However, the 3D image intensities from in-focus areas of a polarimetric material are dependent on the orientation of the polarimetric optical components. The corresponding Stokes parameters will be a non-zero mean Gaussian, [$N(\mu, \sigma^2)$, $\mu \neq 0$]. The Chi distribution is the square root of the sum of squares of a set of independent random variables where each follows a standard normal distribution, [$X = \sqrt{Y_1^2 + \ldots + Y_n^2}$, where $Y_i \sim iid\ N(0,1)$]. Thus, we can distinguish the 3D polarimetric properties in the scene by analyzing the probability distribution of the numerator of *DoP* with each Stokes parameter normalized by its standard deviation:

$$X_z = \sqrt{\sum_{i=1}^{3}(S_i^z/\sigma_i)^2}, X_z \sim Chi\ distribution, if\ S_i^z \sim N(0, \sigma_i^2). \qquad \textbf{(5)}$$

3D Stokes parameters ($S_i^z$, $i$ = [1, 2, 3]) are subtraction of two orthogonal 3D polarimetric images [Eq. 1]. Applying $S_i^z$ to Eq. (5), $X_z$ ~ Chi distribution if $S_i^z$ are measured from an out-of-focus depth ($z$) and/or non-polarimetric material area, and $S_i^z \sim N(0, \sigma_i^2)$ due to the subtraction of two image intensities. Specifically, when measuring the linear polarized property, $S_3$=0 (no circular polarization), and $X_z$~Chi distribution has two degrees of freedom, which is the Rayleigh distribution. $X_z$ will not follow a Chi distribution when $S_i^z$ are measured from an in-focus depth of polarimetric material [$S_i^z \sim N(\mu, \sigma_i^2)$, $\mu \neq 0$]. Total variation denoising algorithm [9] is applied in the 3D *DoP* images to further reduce the effect of noise.

A 3D polarimetric InIm experiment was performed in low light

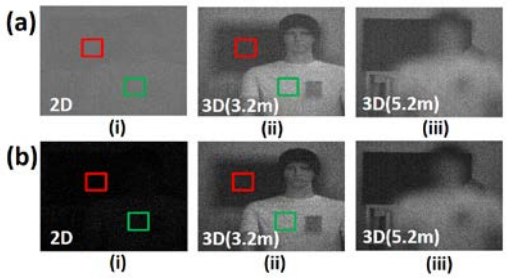


Fig. 2. Conventional InIm in low light. (a) Images with camera offset ($N_{offset}$). (b) Images without $N_{offset}$. (i) Sample 2D perspective image. (ii) 3D image focused on object plane. (iii) 3D image focused on background. Green and red windows correspond to object and background areas for calculation of SNR.

environment. A Hamamatsu C11440-42U camera with Scientific CMOS (SCMOS) image sensor FL-400 was used for SAII. The image sensor has 2048 (H) × 2048 (V) pixels, with a pixel size of 6.5 (H) × 6.5 (V) μm. The exposure time was set as 10 ms. Focal length of the camera was 50 mm. In the experiment, a mannequin with an attached piece of linear polarizer film was placed around 3.2 meters from the camera, and the background is around 5.2 meters away. SAII was preformed using a moving camera with a total of 49 [7(H)×7(V)] perspectives. The pitch between adjacent perspectives is 30 mm in both the horizontal and vertical directions. As circularly polarized light rarely occurs in nature and the material used in the scene has only linear polarization properties, the Stokes parameter ($S_3$) corresponding to circular polarization should be 0. We can simplify the measurement of linear polarization parameters ($S_i, i$=[0, 1, 2]), and only 4 polarimetric images ($I^p, p = \alpha°, \alpha = [0, 45, 90, 135]$)are required at each perspective.

The captured 2D images and 3D reconstructed images using conventional InIm under low illumination are shown in Fig. 2a (i) and Fig. 2a (ii-iii), respectively. Fig. 2b depicts the results when the camera offset ($N_{offset}$) is subtracted from the 2D images. 100 bias reference frames ($bias_k, k = [1, 2, \ldots, 100]$) were recorded by setting a minimum camera exposure time (3ms), with a maximum camera f-stop. An example of the generated 2D image ($\xi$) without $N_{offset}$ is shown in Fig. 2b(i). In addition, this image can be used to estimate the number of photons arriving on the image sensor. The gray scale intensity of the image is first converted to electrons by the conversion factor of the sensor. Number of photons for each pixel is then derived by dividing the converted electrons with the sensor's quantum efficiency: $\gamma = \xi \times CF/QE$ where $\gamma$ is the estimated number of photons, $CF$ = 0.46 electrons/count is the conversion factor, and $QE$ = 70% is quantum efficiency. In Fig. 2b(i), an average of 2.13 photons/pixel are estimated in low illumination condition.

After removing the camera offset, the polarimetric 2D images ($\xi^p_{m,n}$) are applied to the SAII reconstruction algorithm. Figures 2 b(ii) and (iii) illustrate the 3D images at 3.2 m and 5.2 m, respectively. Image SNR is used to compare the 2D and 3D image

**Table 1. SNR measurements between 2D and 3D imaging with or without camera offset ($N_{offset}$). Estimated photons/pixel = 2.13.**

| | 2D image | | 3D image (3.2 m) | |
|---|---|---|---|---|
| | With $N_{offset}$ | No $N_{offset}$ | With $N_{offset}$ | No $N_{offset}$ |
| SNR | 0.71 | 0.73 | 4.93 | 5.14 |

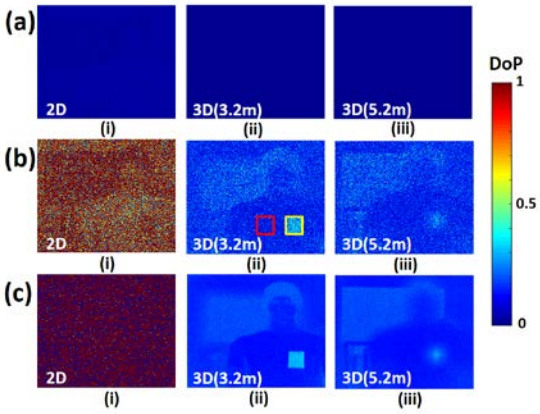


Fig. 3. 2D and 3D *DoP* images. (a) with camera offset ($N_{offset}$), (b) without $N_{offset}$, and (c) without $N_{offset}$ and by applying total variation algorithm. (i) 2D *DoP*. (ii) 3D *DoP* at $z$ = 3.2 m. (iii) 3D *DoP* at $z$ = 5.2m. Yellow and red windows correspond to the polarimetric and non-polarimetric material areas. Estimated photons/pixel = 2.13.

qualities. We define $SNR = (\mu_s - \mu_n)/\sqrt{\sigma_s^2 + \sigma_n^2}$, where $\mu_s, \mu_n$ are the mean value of signal (object), and background areas, respectively. $\sigma_s^2$ , $\sigma_n^2$ are the variances of signal and background areas, respectively. The signal and background pixels were selected within the green and red windows, [Fig. 2], with each having an identical window size. Table 1 illustrates the SNR between the conventional 2D and 3D images in low illumination condition. The 3D image without camera offset has a SNR of 5.14.

Fig. 3 shows the experimental results of the calculated *DoP* images between the proposed approach and conventional 2D methods. Using the images with camera offset ($N_{offset}$), values of 2D *DoP* [Fig. 3a (i)], and 3D *DoP* [Figs. 3a (ii) and (iii)] are close to 0. In low light, the effect of $N_{offset}$ is substantial. The numerator of *DoP* contains photon counts from the scene, but the denominator is dominated by electron counts mainly from $N_{offset}$. Thus, *DoP* cannot reveal accurate polarimetric information. By removing $N_{offset}$, the adjusted polarimetric images may contain zero or negative digitized values, and the corresponding 2D *DoP* may be saturated (*DoP* >1 or <0) [Fig. 3b(i)]. The 3D *DoP* image reduces read noise and can mitigate the saturation effect; however, it is still noisy as shown in Figs. 3b (ii) and (iii). We apply total variation (TV) denoising algorithm [9] to 3D *DoP* images [Figs. 3c (ii) and (iii)]. The reconstructed objects in both depths (3.2 m and 5.2 m) are sharpened while the edges are preserved. The 2D *DoP* with TV [Fig. 3c(i)] cannot provide the correct polarimetric information, which illustrates the advantage of the proposed 3D polarimetric approach.

We quantitatively analyzed the *DoP* images by measuring the SNR as shown in Table 2. In the analysis, the signal was selected as the area of the polarimetric material [see yellow window in Fig. 3b(ii), where a piece of linear polarizer film is placed on the mannequin]. The noise was selected as the non-polarimetric

**Table 2. SNR of the *DoP* images for 2D and 3D polarimetric images with and without camera offset ($N_{offset}$), and with TV denoising algorithm. Estimated photons/pixel = 2.13.**

| | 2D *DoP* | | 3D *DoP* (at 3.2meters depth) | | |
|---|---|---|---|---|---|
| | $N_{offset}$ | No $N_{offset}$ | $N_{offset}$ | No $N_{offset}$ | No $N_{offset}$ + TV |
| SNR | -0.19 | NaN | 0.50 | 1.27 | 7.39 |

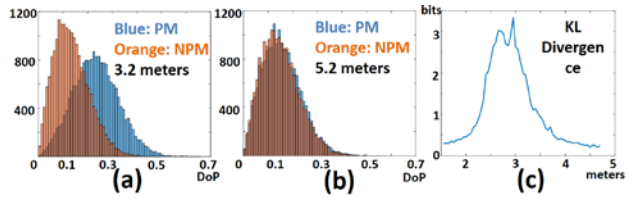


Fig. 4. Histograms of 3D *DoP* numerator [Eq. 5] at (a) 3.2 m focused on object, and (b) 5.2 m (background). PM = polarimetric material, NPM = non-polarimetric material. Estimated photons/pixel = 2.13. Windows [Fig. 3b(ii)] were selected on areas corresponding to the PM area (yellow box), and NPM area (red box). (c) Kullback-Leibler Divergence between the windows along depth range *Z*.

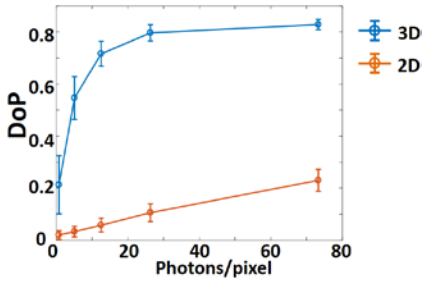


Fig. 5. Mean and standard deviation of *DoP* of polarimetric material area for 3D polarimetric InIm (focused on object) and 2D polarimetric imaging with varying levels of illumination.

material of the T-shirt [red window in Fig. 3b(ii)]. The selected windows have an identical size, and their depth is 3.2 meter from camera. The SNR of the 2D *DoP* [Fig. 3a(i)] generated by the 2D image with $N_{offset}$ is negative with a value of -0.19. The saturated 2D *DoP* [Fig. 3b(i)] provides a SNR value which is not reliable. The 3D *DoP* at 3.2 meters with $N_{offset}$ [Fig. 3a(ii)] and without $N_{offset}$ [Fig. 3b(ii)] have SNR values of 0.50 and 1.27, respectively. With the proposed approach, the SNR in our experiments achieves a maximum of 7.39 as shown in Fig. 3c (ii). The theoretical and experimental results show that the proposed 3D polarimetric InIm can significantly improve *DoP* image quality.

We apply Kullback-Leibler Divergence to measure the relative entropy of probability distributions of 3D *DoP* ($X_z$) [Eq. 5] between signal $[p_s^z(\varphi)]$ and noise $[p_n^z(\varphi)]$, along the reconstruction depth range ($Z$) to illustrate the reduction in noise using our polarimetric approach. The signal is defined to be the polarimetric material area, and noise is for non-polarimetric material. The KL Divergence indicates the difference between two probability distributions:

$$D_{KL}[p_s^z(\varphi), p_n^z(\varphi)] = \sum_{\varphi\in\psi}\{p_s^z(\varphi) log_2[p_s^z(\varphi)/p_n^z(\varphi)]\}, \quad \textbf{(6)}$$

where $D_{KL} \geq 0$, and $D_{KL} = 0$ if $S$=$N$. The depth of polarimetric material is statistically extracted when $D_{KL}$ between polarimetric and non-polarimetric areas reaches a maximum over $Z$:

$$z_p = \underset{z\in Z}{arg\,max}\ \{D_{KL}[p_s^z(\varphi), p_n^z(\varphi)]\}. \quad \textbf{(7)}$$

Figure 4(a)-(b) illustrates the histograms of the random variables derived from the 3D *DoP* numerator [Eq. 5] at 3.2 m and 5.2 m, respectively. The windows were selected in areas of polarimetric material (PM), and non-polarimetric material (NPM) of the scene. Fig. 4(c) depicts the KL Divergence between the PM and NPM areas along the depth range ($Z$). At focused depth position of ~3.2 m, the random variable probability distribution in the PM area will not follow a Chi distribution, which is different with the NPM area, and the KL divergence reaches a maximum. When the PM is out-of-focus, the corresponding $X_z$ ~ Chi distributed and the KL Divergence approaches 0. Note that we cannot extract 3D polarimetric information from conventional 2D polarimetric imaging in low light conditions. We show experimental results for 3D polarimetric imaging under low illumination with an estimated 2.13 photons per pixel captured by the camera. Figure 5 illustrates the mean and standard deviation of the *DoP* of polarimetric material area for the 3D InIm (focused on object plane) and 2D imaging with varying illumination. In very low illumination (photons/pixel < 20), the calculated 3D *DoP* decreases sharply with large standard deviation because of low SNR and measurement uncertainty due to noise. However, our approach substantially outperforms 2D imaging in terms of extracting depth and polarimetric information.

In summary, we have experimentally and theoretically demonstrated an approach for extracting 3D polarimetric information in extreme low light, and used statistical analysis and dedicated algorithms to reduce uncertainty in the polarimetric measurements and to recover the 3D polarimetric signatures. 3D Stokes polarization parameters and 3D *DoP* images are calculated by reducing camera read noise through dedicated 3D reconstruction algorithms, and are statistically analyzed to obtain 3D polarimetric properties in the scene and for 3D polarimetric visualization. Total variation denoising is utilized to further reduce noise in the 3D *DoP*, and 3D polarimetric information is statistically extracted from the Stokes parameters as verified by the Kullback-Leibler Divergence and Entropy metrics computation and analysis. The proposed 3D InIm approach outperforms 2D polarimetric imaging in low light which performed poorly in these conditions.

We thank Shinji Ohsuka and Hisaya Hotaka for valuable discussions about the sCMOS camera provided by Hamamatsu Photonics K. K.

## References

1. M. Born and E. Wolf, *Principles of optics: electromagnetic theory of propagation, interference and diffraction of light* (Elsevier, 2013).
2. G. Lippmann, J. Phys. Theor. Appl, **7**, 821 (1908).
3. M. Martínez-Corral, and B. Javidi, Adv. Opt. Photonics **10**, 512 (2018).
4. B. Tavakoli, B. Javidi, and E. Watson, Opt. Express **16**, 4426 (2008).
5. S. Kullback, and R. Leibler, Math. S., **22**, 79 (1951).
6. X. Xiao, B. Javidi, G. Saavedra, M. Eismann, and M. Martinez-Corral, Opt. Express **20**, 15481 (2012).
7. A. Carnicer, and B. Javidi, Opt. Express **23**, 6408 (2015).
8. J. S. Jang, and B. Javidi, Opt. Lett. **27**, 1144 (2002).
9. L. Rudin, S. Osher, and E. Fatemi, Physica D. **60**, 259 (1992).

**Full reference of citations**


[1] M. Born, and E. Wolf. Principles of optics: electromagnetic theory of propagation, interference and diffraction of light. (Elsevier, 2013).

[2] G. Lippmann, “Epreuves reversibles donnant la sensation du relief,” J. Phys. Theor. Appl, 7(1), pp.821-825 (1908).

[3] M. Martínez-Corral, and B. Javidi, “Fundamentals of 3D imaging and displays: a tutorial on integral imaging, light-field, and plenoptic systems,” Advances in Optics and Photonics. 10(3), 512-66 (2018).

[4] B. Tavakoli, B. Javidi, and E. Watson, "Three dimensional visualization by photon counting computational Integral Imaging," Opt. Express 16, 4426-4436 (2008).

[5] S. Kullback, R. Leibler, “On information and sufficiency,” The annals of mathematical statistics. 22(1), 79-86 (1951).

[6] X. Xiao, B. Javidi, G. Saavedra, M. Eismann, and M. Martinez-Corral, “Three-dimensional polarimetric computational integral imaging,” Optics express 20(14), 15481-8 (2012).

[7] A. Carnicer, and B. Javidi, “Polarimetric 3D integral imaging in photon-starved conditions,” Optics express, 23(5), 6408-17 (2015).

[8] J. S. Jang, and B. Javidi, “Three-dimensional synthetic aperture integral imaging,” Optics letters 27(13), 1144-1146 (2002).

[9] L. Rudin, S. Osher, and E. Fatemi, “Nonlinear total variation based noise removal algorithms,” Physica D: nonlinear phenomena. 60(1–4), 259-268 (1992).